

# Investigation of Stiffening Effects on Notch Growth Trajectory of Composite Stiffened Panels with Large Transverse Notches

Patrick Enjuto,<sup>1</sup> Mark Lobo,<sup>2</sup> and Thomas H. Walker<sup>3</sup>  
*NSE Composites, Seattle, WA, USA*

Gerardo Peña,<sup>4</sup> and Eric Cregger<sup>5</sup>  
*The Boeing Company, Seattle, WA, USA*

and  
Steven Wanthal,<sup>6</sup>  
*The Boeing Company, Charleston, SC, USA*

**Design of robust aircraft structure requires consideration of the load-carrying capability with large damage. Large notches, typically introduced as machined cracks (aka “notches”) severing a single skin bay and a central stiffening member, are often used to conservatively address the wide range of possible large damage scenarios. The objective of current effort was to explore the viability of developing preliminary laminate-based methods for predicting crack turning at the adjacent stiffener using traditional fracture mechanics concepts.**

## Nomenclature

|                 |   |                                     |
|-----------------|---|-------------------------------------|
| $a$             | = | half crack length                   |
| $A_{beam}$      | = | beam area                           |
| $A_{skin}$      | = | skin area                           |
| $A_{stiffener}$ | = | stiffener area                      |
| $b$             | = | stiffener spacing                   |
| $B$             | = | width                               |
| $C$             | = | compliance                          |
| $E_x$           | = | Young’s modulus in the x-direction  |
| $E_y$           | = | Young’s modulus in the y-direction  |
| $EA$            | = | product of Young’s modulus and area |
| $G$             | = | strain energy release rate          |
| $P$             | = | load                                |
| $R_s$           | = | stiffening ratio                    |
| $ss$            | = | subscript for self-similar          |
| $sp$            | = | subscript for splitting             |
| $t_{flg}$       | = | flange thickness                    |
| $t_{skin}$      | = | skin thickness                      |
| $w_{flg}$       | = | flange width                        |
| $Y$             | = | configuration factor                |
| $Y_{strain}$    | = | strain-based configuration factor   |
| $Y_{stress}$    | = | stress-based configuration factor   |

---

<sup>1</sup> Senior Stress Engineer, NSE Composites, AIAA Senior Member.

<sup>2</sup> Senior Stress Engineer, NSE Composites.

<sup>3</sup> Principal Engineer, NSE Composites, AIAA Member.

<sup>4</sup> Research Engineer, Boeing Research & Technology.

<sup>5</sup> Senior Technical Fellow, Boeing Research & Technology, AIAA Associate Fellow.

<sup>6</sup> Technical Fellow, Boeing Research & Technology, AIAA Senior Member.

- $\epsilon_{cfg}$  = configured strain at maximum load
- $\epsilon_{ucfg}$  = unconfigured strain at maximum load
- $\sigma_{cfg}$  = configured stress at maximum load
- $\sigma_{ucfg}$  = unconfigured stress at maximum load

## I. Introduction

IN composite structures, panels with large notches subjected to loading parallel to the initial notch can present different damage growth trajectories depending on the material, laminate and geometrical configuration. For example, it has been observed that, in tests of tension loaded unstiffened panels with notches, laminates with a large percentage of plies parallel to the load direction present damage growth from the initial notch parallel to the load direction. On the other hand, in the case of quasi-isotropic laminates similar tests can result in damage growth from the initial notch perpendicular to the load direction.

Traditionally, methods addressing the large-notch capability have been limited to the determination of the residual strength of panels exhibiting self-similar damage growth from a sharp notch severing a central stiffener. This is a result of the complexity of simulating the damage growth in cases where the laminate/geometrical configuration results in growth trajectories other than self-similar. As a consequence, the laminate design space is generally limited to those laminates that present self-similar growth.

Since designs that exhibit growth from the initial notch parallel to the load direction can result in residual strengths higher than those that display self-similar growth, methodologies that predict the initiation of crack turning and the associated residual strength are of special interest.

The objective of the current effort was to explore the viability of developing preliminary laminate based methods for predicting crack turning using traditional fracture mechanics concepts. Specifically, the use of such methods in the scenario of a notch that presents self-similar growth from the initial notch and results in the notch turning at the adjacent stiffener is studied in this effort.

## II. Finite Element Methodology

### A. Modeling Approach

An FE modeling approach using ABAQUS<sup>®</sup> (Reference 1) was used for the development of preliminary methods for predicting crack turning at the adjacent stiffener. Half-symmetric models were used, as shown in Figure 1. This approach includes explicit modeling of the skin and stiffener flanges, but idealizes the stiffener webs and caps as beam elements, as shown in Figure 2. Similar models with no stiffeners were also used for obtaining the unconfigured response.

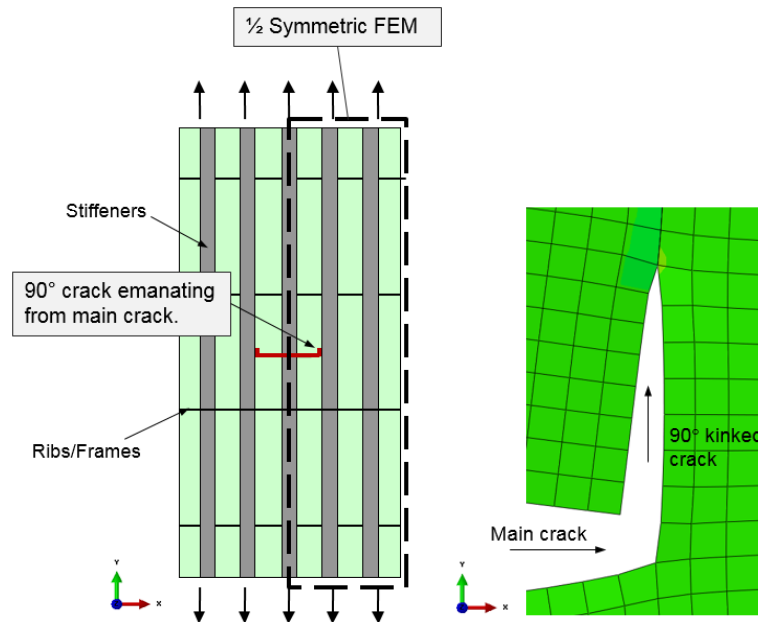
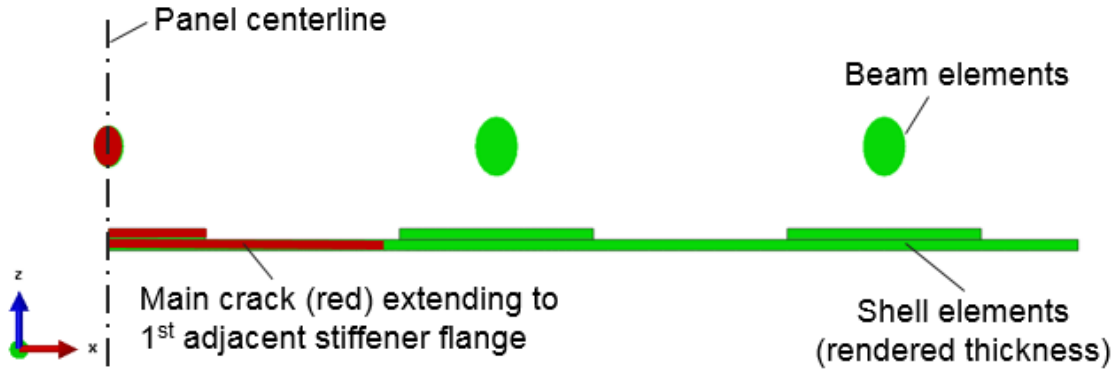


Figure 1. Half-Symmetric FE Model.



**Figure 2. Detail of Modeling Approach Showing Beam Element Representing the Web and Cap of the Stiffener.**

The skin was modeled using shell elements (S4) with a single element through the thickness. The stringer caps and webs were modeled using linear Timoshenko beam elements (B31), and skin-flanges were each modeled with a single S4 shell element through-the-thickness. The geometry modeled did not include chamfers on the attached stringer flanges, corner radii of the stringer channels, or noodles.

To avoid potential inaccuracies in strain energy release rate calculations, the minimum distance between the flange edge and the turning location was set to 1/8" (see Figure 3).

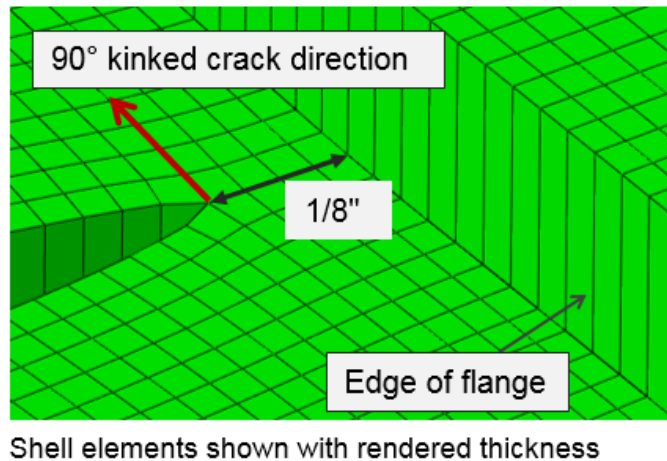


**Figure 3. Kinked crack position.**

## **B. Boundary Conditions**

The model boundary conditions and loading are illustrated in Figure 4. The frames were simulated using a combination of boundary conditions and constraint equations. Specifically, the frames closest to the crack were idealized by constraining the out-of-plane ( $U_z$ ) and transverse ( $U_x$ ) displacements to be zero. The frames closest to the load introduction were idealized by constraining the transverse displacements to be zero and using constraint equations requiring identical out-of-plane displacements. Symmetry conditions were used along the longitudinal panel centerline.

The model was loaded using uniform displacement of all skin and stringer nodes along the loading ends resulting in tension load on the panel. Additionally, transverse and out-of-plane displacements as well as rotations were constrained on that end.

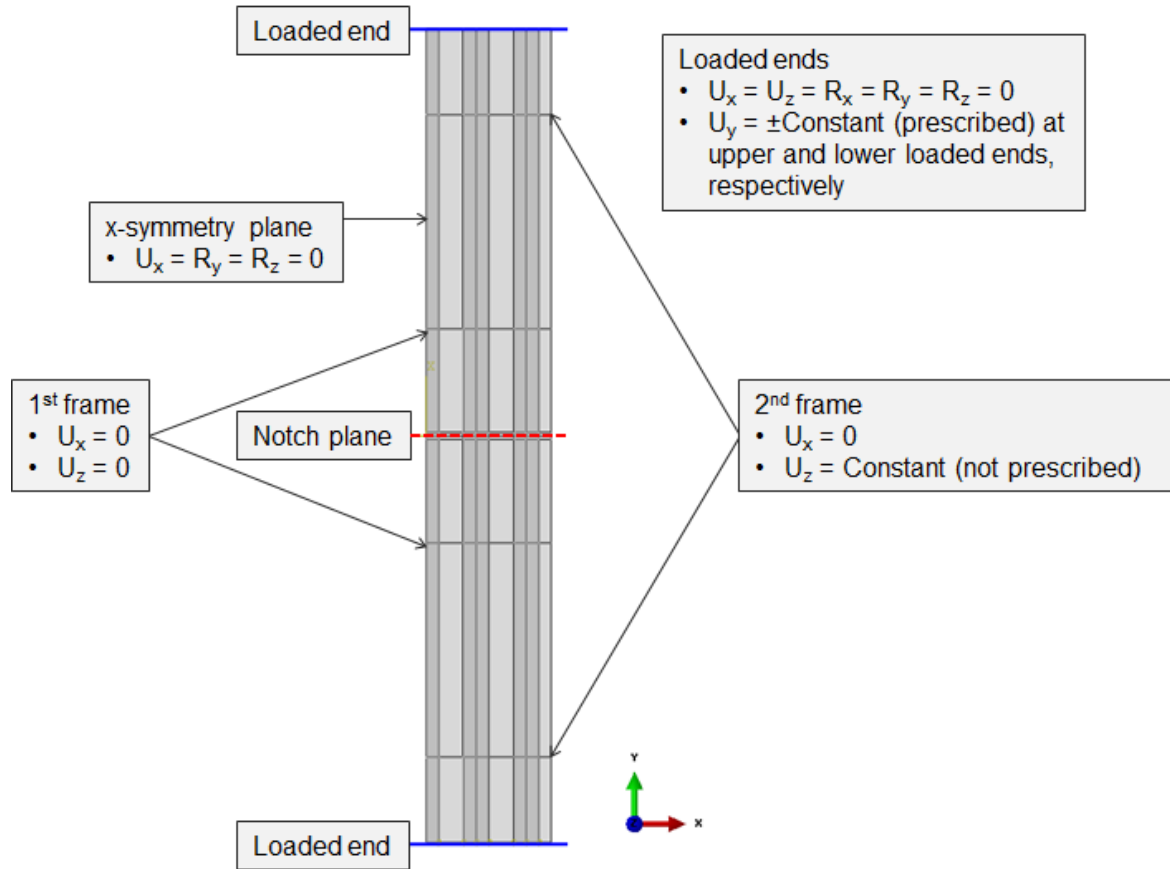


Figure 4. Boundary Conditions.

### III. Approach

The effect of the panel configuration on its large-notch residual strength has often been assumed to be independent of the skin fracture response. With this assumption, the configured panel strength (calculated as the maximum panel load divided by the gross cross-sectional area of the panel) is then determined by applying a configuration (Y-) factor to the strength (far-field failure stress) of a flat, unstiffened panel of the skin material/layout with a notch of the same length (unconfigured strength).

$$\sigma_{cfg} = \frac{\sigma_{ucfg}}{Y_{stress}} \quad (1)$$

Similarly, a strain-based configurational factor can be analogously defined as:

$$\epsilon_{cfg} = \frac{\epsilon_{ucfg}}{Y_{strain}} \quad (2)$$

A direct assessment of the propensity of a stiffened panel configuration for crack turning could be made if, for a given panel, the configured strengths associated with initiation of splitting growth ( $\sigma_{cfg,sp}$ ) and self-similar growth ( $\sigma_{cfg,ss}$ ) were known. The actual damage trajectory would then simply be that of the path of least resistance under the same loading condition (e.g., self-similar growth if,  $\sigma_{cfg,sp} > \sigma_{cfg,ss}$ ). Making use of this concept, in conjunction with the definition of configurational factors, it is possible to obtain a measure of the effect of configuration on the propensity of a crack to turn as:

$$\frac{\sigma_{cfg,ss}}{\sigma_{cfg,sp}} = \frac{\sigma_{ucfg,ss} / Y_{stress,ss}}{\sigma_{ucfg,sp} / Y_{stress,sp}} \Rightarrow \frac{\sigma_{cfg,ss}}{\sigma_{cfg,sp}} = \frac{\sigma_{ucfg,ss}}{\sigma_{ucfg,sp}} \cdot \frac{Y_{stress,sp}}{Y_{stress,ss}} \quad (3)$$

The measure of the effect of configuration on the propensity of a crack to turn would be given by the ratio of the configurational factors (Y-factors) for each of the possible damage trajectories ( $Y_{stress,sp} / Y_{stress,ss}$ ).

Based on this approach a crack would be predicted to turn at the adjacent stiffener if  $\sigma_{cfg,ss} / \sigma_{cfg,sp} > 1.0$ , when the front of the crack is in the vicinity of the adjacent stiffener.

If the self-similar unconfigured strength is greater than the splitting unconfigured strength at splitting initiation, then the skin would be predicted to split without the presence of stiffeners. Therefore, splitting would be expected to occur from an “initial notch” with the notch tip in the skin bay. As a preliminary check to account for this situation, a crack could be predicted to turn from the initial notch if:  $\sigma_{ucfg,ss} / \sigma_{ucfg,sp} > 1.0$ .

Based on evaluation of the FE analysis results, it was observed that the growth of a “kinked” crack emanating at 90° from the main crack (original notch) in the vicinity of the adjacent intact stiffener flange presents a mixed-mode response. For the purposes of this study, growth of the “kinked” crack was assumed to be dominated by Mode II growth since there is no data to support the use of mixed-mode criteria such as the BK or Power laws at this time. As a result of this, and the relationship between energy release rate (G) and applied load (P), a strain configurational factor can be expressed (assuming no configurational dependence of the change in compliance, C, with crack length, a) as:

$$G = \frac{P^2}{2 \cdot B} \cdot \frac{\partial C}{\partial a} \Rightarrow P \propto \sqrt{G} \Rightarrow Y_{strain,sp} = \sqrt{\frac{G_{II,cf g}}{G_{II,ucfg}}} \quad (4)$$

The strain energy release rates were calculated from the NFORC, crack opening displacements, element edge length, and shell thickness using the crack-closure technique, see Reference 2.

#### IV. Results

In order to evaluate the effect of configuration on the propensity of a notch to turn at the adjacent stiffener a series of geometrical configurations were analyzed using FE. Table 1 and Figure 5 provide the key variables associated with the 16 configurations analyzed. In the analyses, representative carbon-epoxy composite laminate material properties were used for all panels (i.e.,  $E_{x,skin} = 7.7$  msi,  $E_{y,skin} = 6.9$  msi,  $E_{x,stiffener} = 13.0$  msi,  $E_{y,stiffener} = 4.5$  msi), and all stiffeners within a single panel were assumed to be identical. Note that  $R_s$  is the stiffening ratio, defined as  $EA_{stiffener} / EA_{skin}$ .

| Panel ID | $t_{flg}$<br>(in) | $t_{skin}$<br>(in) | $b$<br>(in) | $W_{flg}$<br>(in) | $A_{beam}$<br>(in <sup>2</sup> ) | $R_s$ |
|----------|-------------------|--------------------|-------------|-------------------|----------------------------------|-------|
| 101      | 0.2               | 0.2                | 7           | 3.5               | 0.66                             | 1.63  |
| 102      |                   |                    |             |                   | 1.32                             | 2.43  |
| 103      |                   |                    | 12          | 6.0               | 1.16                             | 1.66  |
| 104      |                   |                    |             |                   | 2.32                             | 2.47  |
| 105      |                   | 0.6                | 7           | 3.5               | 0.66                             | 0.54  |
| 106      |                   |                    |             |                   | 1.32                             | 0.81  |
| 107      |                   |                    | 12          | 6.0               | 1.16                             | 0.55  |
| 108      |                   |                    |             |                   | 2.32                             | 0.82  |
| 109      | 0.4               | 0.2                | 7           | 3.5               | 1.24                             | 3.04  |
| 110      |                   |                    |             |                   | 2.48                             | 4.54  |
| 111      |                   |                    | 12          | 6.0               | 2.24                             | 3.18  |
| 112      |                   |                    |             |                   | 4.48                             | 4.76  |
| 113      |                   | 0.6                | 7           | 3.5               | 1.24                             | 1.01  |
| 114      |                   |                    |             |                   | 2.48                             | 1.51  |
| 115      |                   |                    | 12          | 6.0               | 2.24                             | 1.06  |
| 116      |                   |                    |             |                   | 4.48                             | 1.59  |

**Table 1. FE analysis configuration definition.**

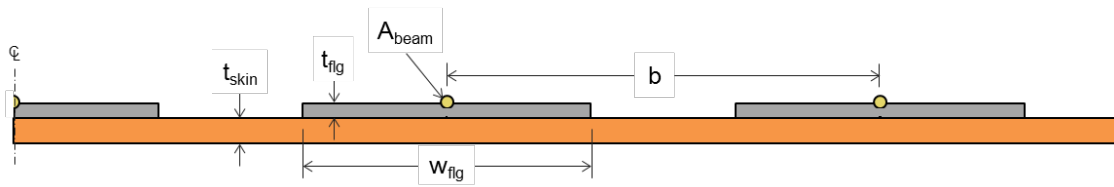


**Figure 5. Variable definition of FE analysis configurations.**

Based on the relationship in Equation (4), strain configurational factors were determined by comparing configured panel FE results with the associated unconfigured panel FE results, and are shown in Figure 6 as a function of stiffening ratio. The strain configurational factors are observed to be within 10% of 1.0.

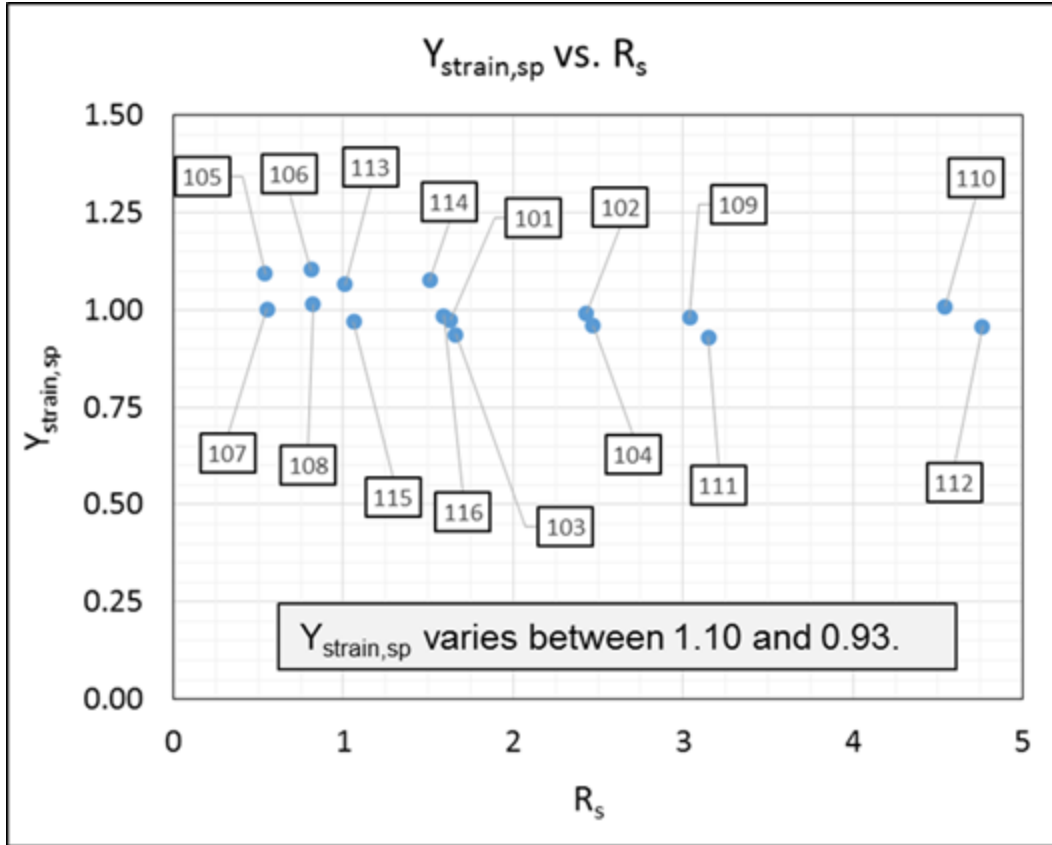


**Figure 6. Strain Configuration Factor vs. Stiffening Ratio.**

A response surface for the stress configurational factor was developed making use of the relationship between stress and strain configurational factors and assuming that  $Y_{strain,sp} = 1.0$ .

$$Y_{stress,sp} = \cancel{Y_{strain,sp}}^1 \cdot \frac{\left(1 + \frac{A_{stiffener}}{A_{skin}}\right)}{(1 + R_s)} = \cancel{Y_{strain,sp}}^1 \cdot \frac{\left(1 + R_s \cdot \frac{E_{skin}}{E_{stiffener}}\right)}{(1 + R_s)} \quad (5)$$

Figure 7 contains Y-factors calculated using the response surface in Equation (5) and the FE analysis results; very good agreement (within 10%) is observed.

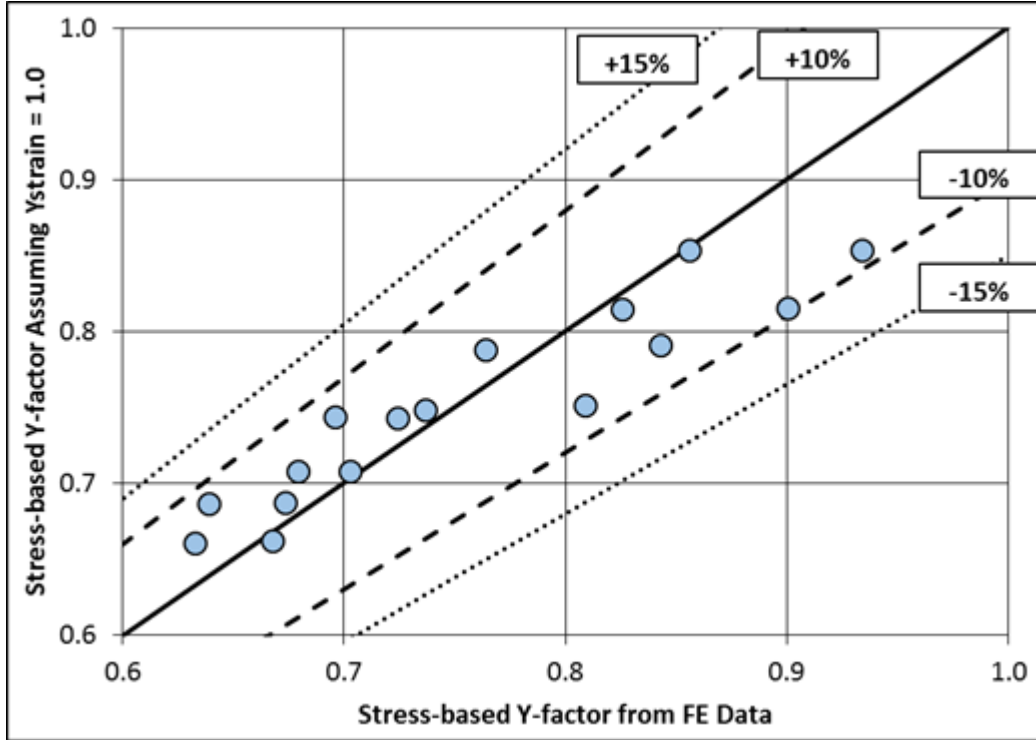


**Figure 7. Stress Configuration Factor Response Surface vs. FE Data.**

As discussed previously, a measure of the effect of configuration on the propensity of a crack to turn can be obtained from the ratio  $Y_{stress,sp} / Y_{stress,ss}$  in:

$$\frac{\sigma_{cfg,ss}}{\sigma_{cfg,sp}} = \frac{\sigma_{ucfg,ss}}{\sigma_{ucfg,sp}} \cdot \frac{Y_{stress,sp}}{Y_{stress,ss}} \quad (6)$$

The self-similar and splitting capabilities should be calculated for the same configuration, i.e. when the original crack has extended to the adjacent stiffener. Nominally, both the splitting and self-similar capability should be associated with initiation of additional growth, not final 2-piece failure. In the current work, the splitting unconfigured strength ( $\sigma_{ucfg,sp}$ ) and configurational factor ( $Y_{stress,sp}$ ) are calculated at a notch length of two times the stiffener spacing,  $b$ , minus the flange width, ( $w_{flg}$ ). On the other hand, as an approximation for the purposes of this study, the self-similar unconfigured strength ( $\sigma_{ucfg,ss}$ ) and configurational factor ( $Y_{stress,ss}$ ) are assumed as those associated with two-piece failure. As such,  $\sigma_{ucfg,ss}$  is calculated using the unconfigured strength at a notch length of two times the stiffener spacing ( $b$ ), and  $Y_{stress,ss}$  is that given in Reference 3.

A comparison of the  $Y_{stress,ss}$  response surface developed in Reference 3 and the  $Y_{stress,sp}$  response surface developed in this effort is shown in Figure 8. A measure of the effect of configuration on the propensity of a crack to turn is given by the ratio of the configurational factors (Y-factors) for each of the possible damage trajectories ( $Y_{stress,sp} / Y_{stress,ss}$ ). With the approximations given in the previous paragraph, for the configurations under study the comparison of the splitting and self similar Y-factors indicates that the unconfigured splitting strength needs to be no more than 14-24% higher than the unconfigured self-similar strength for a self-similar crack to be predicted to turn at the adjacent stiffener.

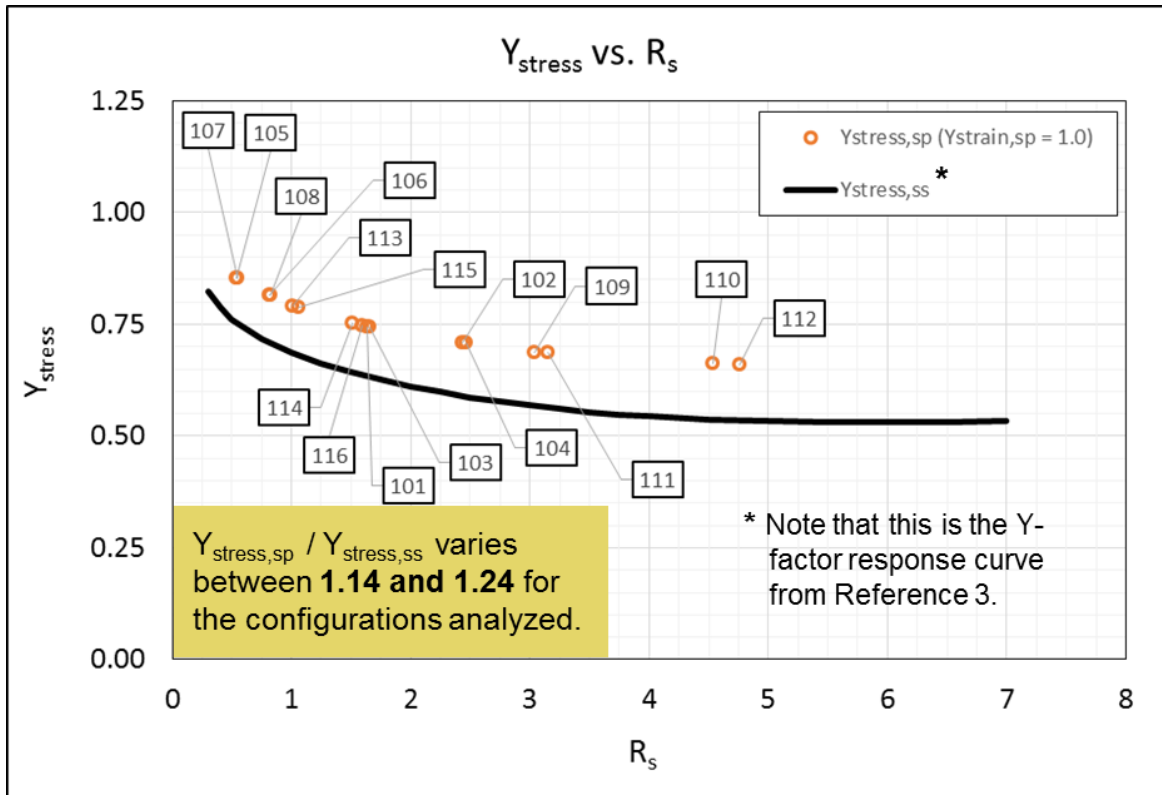


**Figure 8. Stress Configuration Factor vs. Stiffening Ratio.**

## V. Conclusion

In summary, a laminate-based FEA methodology for the analysis of a kinked crack emanating at  $90^\circ$  from the original notch in the vicinity of the adjacent intact stiffener flange was developed following traditional fracture mechanics approaches. Configuration factors for splitting of the  $90^\circ$  crack ( $Y_{\text{stress,sp}}$ ) were determined by comparing configured panel results with the associated unconfigured panel results. Due to the lack of test data, and based on engineering judgement, the growth of the “kinked” crack was assumed to be driven by pure Mode II.

Based on the ratio of the configuration factors for splitting and self-similar growth, together with the ratio of the unconfigured strength for each mode, a preliminary method for predicting the initiation of crack turning at the adjacent intact stiffener was developed. Based on the results from simplified FE analyses for a limited design space, this preliminary approach for predicting crack turning propensity at the first adjacent stiffener in configured panels appears to provide a reasonable framework but significant further development is necessary in order to reach a level of maturity compatible with industry usage for preliminary design.

## Acknowledgements

The material is based upon work supported by NASA under Award Nos. NNL09AA00A and 80LARC17C0004.

## References

- <sup>1</sup>ABAQUS®, Software Package, Ver. 6.14-1, Dassault Systèmes Simulia Corporation, Waltham, MA, 2014.
- <sup>2</sup>Krueger, R., "The Virtual Crack Closure Technique: History, Approach and Applications," NASA Contractor Report NASA/CR-2002-211628, April 2002.
- <sup>3</sup>Enjuto, P., Walker, T., Lobo, M., Cregger, E., and Wanthal, S. "Investigation of Stiffening and Curvature Effects on the Residual Strength of Composite Stiffened Panels with Large Transverse Notches", 2018 AIAA/ASCE/AHS/ASC Structures, Structural Dynamics, and Materials Conference, AIAA SciTech Forum, (AIAA 2018-2251).